NASA

Technical Memorandum 79617

An Evaluation of the First Four Landsat-D Thematic Mapper Reflective Sensors for Monitoring Vegetation: A Comparison with Other Satellite Sensor Systems

Compton J. Tucker

May 1978

National Aeronautics and
Space Administration

Goddard Space Flight Center
Greenbelt, Maryland 20771

TM 79617

AN EVALUATION OF THE FIRST FOUR LANDSAT-D THEMATIC MAPPER REFLECTIVE SENSORS FOR MONITORING VEGETATION: A COMPARISON WITH OTHER SATELLITE SENSOR SYSTEMS

Compton J. Tucker
Earth Resources Branch, Code 923

May 1978

GODDARD SPACE FLIGHT CENTER
Greenbelt, Maryland 20771 USA

TABLES

ILLUSTRATIONS

AN EVALUATION OF THE FIRST FOUR LANDSAT-D THEMATIC MAPPER REFLECTIVE SENSORS FOR MONITORING VEGETATION: A COMPARISON WITH OTHER SATELLITE SENSOR SYSTEMS

The use of Landsat multispectral scanner (MSS) data for monitoring vegetation has provided a new tool for resource managers. The successful applications of these data are too numerous to review and interested readers are directed to various survey documents such as the NASA ERTS Symposiums (1973a and 1973b), Williams and Carter (1976), and Short et al. (1976).

It should be remembered, however, that the MSS is a first generation orbital remote sensing device. It appears quite curious that the bands are: 0.50 - 0.60, 0.60 - 0.70, 0.70 - 0.80, and 0.80 - 1.10 μm. Immediately questions spring to mind regarding at least slight wavelength or bandwidth changes for various applications.

Several workers in the remote sensing of vegetation field have suggested what they consider to be more suitable bands for monitoring vegetation. Tucker and Maxwell (1976) evaluated the RBV and MSS bands for Landsat using narrow bandpass in situ collected spectral reflectances from the 0.35 - 1.00 μm region. They concluded that three spectral regions of strong and persistant statistical significance existed for this region: 0.37 - 0.50, 0.63 - 0.69, and 0.74 - 1.00 μm.

Other workers have also looked at the questions of sensor selection for monitoring vegetation using different approaches. Gausman et al. (1973) investigated leaf spectra and found that the wavelengths of 0.68, 0.85, 1.65 and 2.20 μm were useful for monitoring vegetation.

Kondratyev et al. (1973) reported the most informative spectral intervals for the monitoring of natural materials were 0.54 - 0.56, 0.66 - 0.68, and 0.78 - 0.82 μm. In a subsequent article, Kondratyev et al. (1975) conclude that three main informative sections of the spectrum can be distinguished and are 0.83 - 0.85, 0.63 - 0.69, and 0.40 - 0.44 μm.

PROPOSED SECOND GENERATION SATELLITE SENSOR SYSTEMS

Colvocoresses' Operational Landsat

Colvocoresses (1977) has proposed a three band sensor system for an "operational Landsat". This system would have bands at 0.47 - 0.57, 0.57 - 0.70, and 0.76 - 1.05 μm having 60 to 90, 30 to 40, and 60 to 90 m resolution, respectively. Sensors would use multilinear array (MLA) technology, which, at the present, limits these devices to the 0.40 - 1.05 μm spectral region. These proposed sensors will be evaluated in this paper.

SPOT

The French Centre National d'Etudes Spatial (CNES) has scheduled a three-band MLA satellite designed Systems Probatoire d'Observation de la Terre (SPOT) for launch in 1983. Three reflective bands are proposed: 0.50 - 0.59, 0.61 - 0.69, and 0.79 - 0.90 μm with 20 m spatial resolution each. Radiometric resolution would be eight bits (256 quantizing levels) (CNES, 1978). The three SPOT bands will be evaluated in this paper.

Landsat-D

It became apparent, with the successes of Landsat-1, that a more suitable and second generation space flown scanner system would provide superior remotely sensed data from vegetated targets. A satellite dedicated to and designed for vegetational monitoring was recommended by the National Academy of Science (CORSPERS, 1976). Christened Landsat-D, designed primarily for vegetational applications, and scheduled for launch in 1981, this mission is to fly a new multispectral scanner system called the thematic mapper (TM).

Specific improvements over the MSS of the first three Landsats have been achieved in the areas of spatial, spectral, and radiometric resolution. Specifically, the IFOV will be 30 m, there will be seven spectral bands, and the TM will have eight bit data vs. six bit data for the MSS (i.e., 256 quantizing levels vs. 64 quantizing levels, respectively). In addition, the spectral channels have been chosen to maximize the information context for green vegetation (Table 1).

CONSIDERATIONS IN SENSOR SELECTION

Remote sensing of vegetation has the objective of monitoring vegetation using reflected or emitted electro-magnetic radiation. Heretofore, most efforts in this regard have used the 0.40 - 2.50 μm region with the major effort occurring in the 0.40 - 1.10 μm area.

Engineers charged with the task of designing a space-flown remote sensing instrument are usually faced with the situation of only being able to accommodate a small number of bands. This results from the design criteria of complexity,

Table 1

Thematic Mapper Spectral and Radiometric Characteristics

Band	Wavelength (μm)	NE $\Delta\rho$	Basic Primary Rationale for Vegetation
TM 1	0.45 - 0.52	0.008	Sensitivity to chlorophyll and carotinoid concentrations
TM 2	0.52 - 0.60	0.005	Slight sensitivity to chlorophyll plus green region characteristics
TM 3	0.63 - 0.69	0.005	Sensitivity to chlorophyll
TM 4	0.76 - 0.90	0.005	Sensitivity to vegetational density or biomass
TM 5	1.55 - 1.75	0.01	Sensitivity to water in plant leaves
TM 6	2.08 - 2.35	0.024	Sensitivity to water in plant leaves
TM 7	10.4 - 12.5	0.5 K	Thermal properties

signal/noise ratios, detector response, energy needs, weight, reliability, data processing and storage considerations, atmospheric effects, etc. The decision must then be made to allocate these sensors in such a fashion to maximize the information content for the application in question.

I will now consider the reflective region of the spectrum (0.35 - 2.50 μm) and discuss various spectral intervals which express different information about vegetated surfaces. Previous basic research from physiological perspectives using in situ spectral data and laboratory leaf spectra are in good agreement in these regards. The in situ results will be briefly reviewed as will several of the leaf spectra results. Five primary and two transition regions exist between 0.35 - 2.50μm where different physiological variables control the resulting leaf and/or canopy spectral reflectance:

1. The 0.350 - 0.500 μm region is characterized by strong absorption by the carotenoids and chlorophylls. A strong relationship exists between spectral reflectance in this region and the plant pigments present (Knipling 1970, Woolley 1971, Salisbury and Ross 1969, Tucker 1977).

2. The 0.500 - 0.620 μm region is characterized by a reduced level of pigment absorption. This results in a higher reflectance than the adjacent blue and red regions which our eyes perceive as "green". A weaker relationship exists between spectral reflectance in this region and the plant material present (Knipling 1970, Woolley 1971, Salisbury and Ross 1969).

3. The 0.620 - 0.700 μm region is characterized by strong chlorophyll absorption. A strong relationship exists between spectral reflectance in this region and the chlorophyll present (Knipling 1970, Woolley 1971, Salisbury and Ross 1969, among others).

4. The 0.70 - 0.74 μm region is characterized by the transition from strong chlorophyll absorption (ending at ~0.70 - 0.71 μm) and the high levels of reflectance characteristic of green vegetation which begin at ~0.74 - 0.75 μm. As such, there is a poor relationship (if any) between the amount of green vegetation and reflectance in this region (Tucker and Maxwell, 1976).

5. The 0.74 - 1.10 μm region is characterized by high levels of reflectance occurring in the absence of any absorptance. A strong relationship exists between spectral reflectance in this region and the amount of green vegetation present (Knipling 1970, Woolley 1971, among others).

6. A ~1.1 - 1.3 μm transition must occur between the region of high reflectance (~0.74 - 1.1 μm) and the water absorption region (~1.3 - 2.5 μm). This is hypothesised because there is no experimental data to support this statement.

7. The 1.30 - 2.50 μm region is characterized by strong absorption by water present in the vegetation. A strong relationship exists between reflectances from this interval and the amount of water present in the leaves of the canopy (Knipling 1970, Woolley 1971, among others).

The desire to maximize the information content for reflective remote sensing of vegetation missions then comes down to selecting some ordered list drawn from the previous list of seven (Table 2).

It should be stressed that although the 0.70 - 0.74 and ~1.1 - 1.3 μm regions' reflectances are not directly coupled with green vegetation, valuable spectral information can be remotely sensed in these regions. The spectral information is related more to the background spectra or to other properties of the materials present. The information content is increased when using these indirectly coupled region(s) in conjunction with the highly correlated with green vegetation regions.

Table 2

Ordered List of Spectral Regions in Descending Usefulness for Monitoring Green Vegetation

Number	Wavelength (μm)	Utility for Vegetation
1	0.74 - ~1.1	Direct biomass sensitivity
2	0.63 - 0.69	Direct in vivo chlorophyll sensitivity
3	~1.3 - 2.5	Direct in vivo foliar water sensitivity
4	0.37 - 0.50	Direct in vivo carotinoid and chlorophyll sensitivity
5	0.50 - 0.62	Direct/indirect and slight sensitivity to chlorophyll
6	0.70 - 0.74	Indirect and minimal sensitivity to vegetation; perhaps valuable non-vegetational information
7	~1.1 - 1.3	

Data Used

Thirty-five plots were sampled in June, 1972 and forty plots were sampled in September, 1971. All plots were 1/4 m^2 in area and were composed of blue grama grass. They were sampled in situ by spectroradiometric measurement over the 0.350 - 0.800 μm (September) and the 0.350 - 1.000 μm (June) region at every 0.005 μm interval with the mobile field spectrometer laboratory (Miller et al. 1976). All measurements were made normal to the ground surface.

Immediately after the reflectance measurements were completed, the plot was clipped of all standing vegetation and an aliquot was extracted for chlorophyll analysis. Canopy biological measurements included total wet biomass, total dry biomass, dry green biomass, dry brown biomass, the leaf water content, and chlorophyll content (Table 3).

METHODS AND ANALYSIS

Description of Research Undertaken

The research was undertaken to evaluate the TM sensors by integration of narrow bandwidth ($0.005\,\mu m$) spectral radiance curves. Spectral reflectances were multiplied by a spectral irradiance function resulting in spectral radiances. The spectral irradiance was passed through the atmosphere (horizontal visibility at sea level = 23 km) to sea level where the various spectral radiances were computed by the product of the spectral irradiance and spectral reflectances. The spectral radiances were then passed through the same atmosphere to the correct orbital altitude for the sensor system in question.

The resulting radiances were integrated and subsequently regressed against the total wet biomass, total dry biomass, dry green biomass, dry brown biomass, leaf water content, and total chlorophyll content to quantify the relationship between the simulated sensor and the various basic properties of the vegetation canopy in question (i.e., biomass, water content, chlorophyll content). To give a sound basis for comparisons to other sensor systems, the same

Table 3

Statistical Summary of the Biophysical Characteristics of the Sample Plots. A Statistical Description of the Vegetative Canopy Characteristics for (A) The Thirty-Five 1/4 M^2 Sample Plots of Blue Grama Sampled in June 1972, and (B) The Forty 1/4 M^2 Sample Plots of Blue Grama Sampled in September 1971.

Sample	Range	Mean	Standard Deviation	Coefficient of Variation	Standard Error of the Mean
A. June, 1972					
Wet total biomass (g/m^2)	52.00-1230.40	339.52	316.94	93.35	50.11
Dry total biomass (g/m^2)	13.04- 528.84	134.07	130.25	97.15	20.59
Dry green biomass (g/m^2)	12.48- 343.36	105.11	93.46	88.93	14.78
Dry brown biomass (g/m^2)	00.16- 185.48	28.96	40.23	138.91	6.36
Leaf water (g/m^2)	38.12- 701.56	205.46	187.83	91.42	29.70
Chlorophyll (mg/m^2)	62.27-2108.06	414.41	515.56	124.41	81.52

Table 3 (Continued)

Sample	Range	Mean	Standard Deviation	Coefficient of Variation	Standard Error of the Mean
B. September, 1971					
Wet total biomass (g/m^2)	70.83- 491.22	261.31	134.00	51.44	21.25
Dry total biomass (g/m^2)	41.50- 337.84	168.55	90.81	53.88	14.36
Dry green biomass (g/m^2)	17.12- 185.04	89.38	50.15	56.11	14.36
Dry brown biomass (g/m^2)	20.40- 186.42	82.41	48.54	58.90	7.68
Leaf water (g/m^2)	28.03- 190.80	92.75	50.93	54.91	8.05
Chlorophyll (mg/m^2)	53.02- 778.97	319.58	238.73	74.70	37.75

analysis was completed for the RBV, MSS, the French SPOT System, and Colvocoresses' proposed sensor system.

This research only addresses the question of spectral resolution. The issues of spatial and radiometric resolution are not addressed in this paper. The author realizes that real world comparisons between TM (post 1981) and other sensor system(s) imagery, for example, will effectively be a comparison between the spectral, spatial, and radiometric resolution interaction(s) for these earth resource systems. This study, however, should give insight into the spectral resolution(s) of the various sensor systems for making measurements of vegetation.

Grass canopies are ideally suited for these experimental purposes because of their morphologic simplicity. More importantly, the various sensors are evaluated by their statistical sensitivity to basic properties of terrestrial vegetation (wet biomass, dry biomass, green biomass, brown or dead biomass, leaf water content, and chlorophyll content). The results of this experiment are thus applicable to terrestrial vegetation in general.

Regression Analysis

A regression approach was undertaken to approximate the relationships existing between the six sampled canopy variables (Table 3) and the integrated radiance for each simulated sensor. Four regression models were evaluated for each interval. Standard regression notation after Draper and Smith (1966) will be used and donated as a function of wavelength by the subscript.

$$\text{CANOPY RAD} = \beta_{0\lambda} e^{(\beta_{1\lambda} \cdot \text{ plot variable})} \qquad (1)$$

where:

CANOPY RAD = normal canopy spectral radiance,

$\beta_{0\lambda}$ = estimated value of β_0 at wavelength λ,

$\beta_{1\lambda}$ = estimated value of β_1 at wavelength λ,

e = Napier's number (i.e., ~2.72);

plot variable = total wet biomass, chlorophyll, etc. (see Table 3).

$$\text{CANOPY RAD} = \beta_{0\lambda} + \beta_{1\lambda} \cdot (\text{plot variable})^{-1} \qquad (2)$$

$$\text{CANOPY RAD} = \beta_{0\lambda} + \beta_{1\lambda} \cdot (\text{plot variable}) \qquad (3)$$

and

$$\text{CANOPY RAD} = \hat{S}(1 - e^{(\beta_{0\lambda} + \beta_{1\lambda} \cdot \text{ plot variable})}) \qquad (4)$$

where:

S = asymptotic radiance estimate at wavelength.

Equations (1), (2) and (4) were transformed into linear models prior to regression computation.

Regression screening was used to evaluate the relationship(s) between the various integrated radiances and the canopy biological measurements. In this way comparisons can easily be made between r^2 values to determine spectral sensitivity for a variety of bandwidths with respect to each of the canopy biological measurements.

Sensors Evaluated

The first four TM sensors, the seven RBV and MSS sensors, the three SPOT sensors, and the three proposed operational Landsat sensors were evaluated using the experimental methods described herein. Data limitations prevented any evaluation(s) beyond 1.00 μm for the June data and beyond 0.80 μm for the September data set.

RESULTS AND DISCUSSION

The various simulated sensors (see Table 4) were regressed against the six canopy variables measured for the June and September data sets. This resulted in 192 separate comparisons which are presented in tabular form (Tables 4 and 5).

The June data was almost entirely green with little standing dead vegetation (Table 3). As such, it can be considered analogous to many agricultural situations where the plant canopy is not only homogeneous but in-phase phenologically. The September data, by contrast, can be considered analogous to many agricultural situations where the canopy in question is beginning to enter senescence, has suffered from some stress, or for some reason is composed of appreciable amounts of live and dead material. In addition, the September data set is analogous to many wild or natural ecological situations where the vegetational scene is not homogeneous. These situations usually have a mixture of early maturing, late maturing, etc. species and, regardless of

Table 4
Coefficient of Determination (r^2) Values Resulting from the Regressions Between Integrated Radiance and the Various Sampled Canopy Variables for the June Data

Sensor	Bandwidth (μm)	Total Wet Biomass	Total Dry Biomass	Leaf Water Content	Dry Green Biomass	Dry Brown Biomass	Total Chlorophyll Content
RBV 1	.475 - .575	.73	.66	.76	.67	.24	.77
RBV 2	.580 - .680	.88	.81	.91	.82	.32	.91
RBV 3	.690 - .800	.65	.63	.65	.63	.51	.65
MSS 4	.500 - .600	.78	.71	.81	.73	.27	.81
MSS 5	.600 - .700	.88	.80	.91	.82	.32	.91
MSS 6	.700 - .800	.63	.62	.63	.61	.54	.65
MSS 7*	.800 - 1.100	.72	.71	.73	.71	.61	.73
TM 1	.450 - .520	.69	.61	.72	.63	.19	.74
TM 2	.520 - .600	.70	.72	.82	.74	.28	.83
TM 3	.630 - .690	.88	.80	.91	.82	.32	.91
TM 4	.760 - .900	.78	.76	.78	.76	.63	.78
SPOT 1	0.50 - 0.59	.76	.69	.79	.71	.26	.81
SPOT 2	0.61 - 0.69	.88	.81	.91	.82	.32	.91
SPOT 3	0.79 - 0.90	.77	.75	.77	.75	.63	.78
Colvo 1	.470 - .570	.71	.65	.75	.66	.23	.76
Colvo 2	.570 - .700	.88	.80	.91	.82	.32	.91
Colvo 3*	.760 - 1.050	.74	.73	.74	.72	.62	.75

*Data were incomplete for the 1.00 – 1.1 μm interval. The simulations for MSS7 and Colvo 3 used 1.00 μm as their upper wavelength limits.

Table 5

Coefficient of Determination (r^2) Values Resulting from the Regressions Between Integrated Radiance and the Various Sampled Canopy Variables for the September Data

Sensor	Bandwidth (μm)	Total Wet Biomass	Total Dry Biomass	Leaf Water Content	Dry Green Biomass	Dry Brown Biomass	Total Chlorophyll Content
RBV 1	.475 - .575	.31	.28	.41	.21	.10	.25
RBV 2	.580 - .680	.40	.38	.64	.24	.07	.33
RBV 3	.690 - .800	.48	.51	.41	.43	.29	.39
MSS 4	.500 - .600	.25	.22	.37	.16	.07	.20
MSS 5	.600 - .700	.39	.38	.65	.23	.06	.33
MSS 6	.700 - .800	.53	.55	.48	.47	.30	.44
MSS 7*	.800 - 1.100	--	--	--	--	--	--
TM 1	.450 - .520	.56	.54	.69	.41	.19	.45
TM 2	.520 - .600	.22	.20	.33	.14	.06	.18
TM 3	.630 - .690	.43	.25	.70	.41	.07	.36
TM 4*	.760 - .900	--	--	--	--	--	--
SPOT 1	0.50 - 0.59	.25	.17	.35	.22	.08	.20
SPOT 2	0.61 - 0.69	.42	.24	.68	.41	.07	.35
SPOT 3*	0.79 - 0.90	--	--	--	--	--	--
Colvo 1	.470 - .570	.33	.23	.43	.30	.11	.26
Colvo 2	.570 - .700	.37	.22	.62	.35	.12	.32
Colvo 3*	.760 - 1.050	--	--	--	--	--	--

*The September data only covered the 0.350 – 0.800 μm region. Some sensors, therefore, could not be simulated.

sampling time, have a mixture of live and dead vegetation, several species, and the such.

Interpretations then of the June and September experimental results should give some insight into the phenological utility, natural ecosystem applicability, and quantify the influence of canopy heterogeneity upon the sensors evaluated.

Coupled with the various sensor simulations presented in Tables 4 and 5, are the results of within-sensor integrations for all of the sensors evaluated. Complete tabular results for all sensors evaluated appear in Appendex A.

RBV and MSS

The seven Landsat-1, 2, and 3 reflective RBV and MSS sensors ranged from good to poor in terms of spectral characteristics for monitoring vegetation (Tables 4 and 5).

Specifically, RBV1 (0.475 - 0.575 μm) combines spectral radiances from the 0.500 - 0.575 μm region of lessened significance and does not include enough of the blue region to be effective in a mixed live/dead canopy situation (Table 5). The 0.475 - 0.500 μm region of the spectrum contributes the spectral information that is highly related to plant canopies for RBV1 but this is seriously degraded by the 0.500 - 0.575 μm signal of reduced statistical significance to green vegetation.

RBV2 (0.58 - 0.68 μm) is somewhat better placed spectrally for monitoring green vegetation (Tables 4 and 5). It combines, however, a region of strong in situ chlorophyll absorption (~ 0.62 - 0.68 μm) with an adjacent region of much reduced <u>in situ</u> chlorophyll absorption (~ 0.58 - 0.62 μm). This had little effect for the in-phase phenologically and homogeneous plant canopy scene but reduced the regression significance by 6% for the more complex canopy case (Table 5; leaf water content variable).

RBV3 (0.69 - 0.80 μm) is particularly poorly placed spectrally for monitoring green vegetation. It combines three separate green vegetation-reflectance relationships: the 0.69 - 0.70 μm region of chlorophyll absorption; the 0.70 - 0.74 μm region of lessened statistical significance or noise; and the 0.75 - 0.80 μm region of enhanced reflectance characteristic of green vegetation. As such, RBV3 is seriously degraded by its spectral configuration for any green vegetation application(s).

MSS4 (0.50 - 0.60 μm) is placed in a spectral region where reduced chlorophyll absorption occurs (Salisbury and Ross, 1969). This is advantageous for green vegetation applications because the same relationship exists across the entire bandwidth. Different relationships are not combined for MSS4 as they are for RBV1 and RBV2. Some carotenoid and chlorophyll absorption occur in the 0.50 - 0.52 μm region and this interval should be excluded to more completely exploit the green vegetation-spectral coupling resulting from the reduced chlorophyll and lack of carotenoid absorption present in the 0.52 - 0.60 μm region.

MSS5 (0.60 - 0.70 μm) is situated in a region of strong <u>in vivo</u> chlorophyll absorption. The <u>in vivo</u> absorption maxima occurs in the 0.67 - 0.68 μm region with higher absorption coefficients for the 0.63 - 0.70 than 0.60 - 0.63 μm region (Salisbury and Ross, 1969). As such, MSS5 could be improved by excluding the 0.60 - 0.63 μm region from the 0.63 - 0.70 μm region. This improvement is most apparent for the more complex canopy situation (Table 5).

MSS6 is redundant to MSS7 and includes the noisy 0.70 - 0.74 μm region. The usefulness of MSS6 is thought to result from the 0.75 - 0.80 μm signal's strong relationship to green leaf biomass and the associated high soil-green vegetation reflectance contrast (Tucker and Miller, 1977).

MSS7 receives spectral radiances which are highly and directly related to green leaf density from the 0.80 - 1.10 μm region. A water band situated at 0.92 - 0.98 μm introduces degrading atmospheric effects and filter/detector characteristics sharply reduce the contribution from the 0.95 - 1.10 μm region relative to that from the 0.80 - 0.95 μm interval (Hovis, 1977).

MSS7 is superior to MSS6 for high green biomass situations (reviewed in Tucker, 1979) while MSS6 has been shown to be superior to MSS7 for lower (rangeland) green biomass applications. A hypothesis explaining this has been presented by Tucker and Miller (1977) based upon soil-green biomass reflectance contrasts and is in agreement with several Landsat-1 and 2 results (Maxwell, 1976; Rouse et al., 1974; Deering, 1978).

Colvocoresses' Proposed Satellite Sensor System

Colvocoress (1977) has proposed a three sensor system for an "operational" Landsat system. Evaluation of these sensors was similar to RBV1, RBV 2, and

TM4, respectively for Colvo 1, Colvo 2, and Colvo 3 (Tables 4 and 5). The same criticisms of RBV1 and RBV2 apply to Colvo 1 and Colvo 2.

Specifically, Colvo 1 (0.47 - 0.57 μm) is poorly placed from a vegetational perspective. Spectral radiances from the 0.47 - 0.50 μm region which are highly correlated with the plant pigments present are combined with spectral radiances from the 0.50 - 0.57 μm region which are not highly correlated with green vegetation in a mixed live/dead canopy situation (Tables 4 and 5; Figure 1).

Colvo 2 (0.57 - 0.70 μm) combines the 0.57 - 0.62 μm region of lower regression significance with the highly significant 0.63 - 0.70 μm region resulting in a serious degrading of this sensor for more complex canopy applications (Figure 2).

Colvo 3 (0.76 - 1.05 μm) is similar to TM4 (0.76 - 0.90 μm) except that Colvo 3 includes the water absorption band at ~0.92 - 0.98 μm within the 0.90 - 1.05 μm region. This will restrict signature extention significantly. The sensors Colvocoresses (1977) has proposed are not optimum for satellite remote sensing of vegetation resources. Any data from these hypothetical sensors would not yield satisfactory results for many vegetational applications and would be inferior to the existing MSS data for most vegetational applications (Tables 4 and 5). Detailed vegetational applications require optimum spectral resolution.

<u>Thematic Mapper</u>

TM1 (0.45 - 0.52 μm) is placed to take advantage of the relationship between spectral radiances from vegetation which are determined in part by the

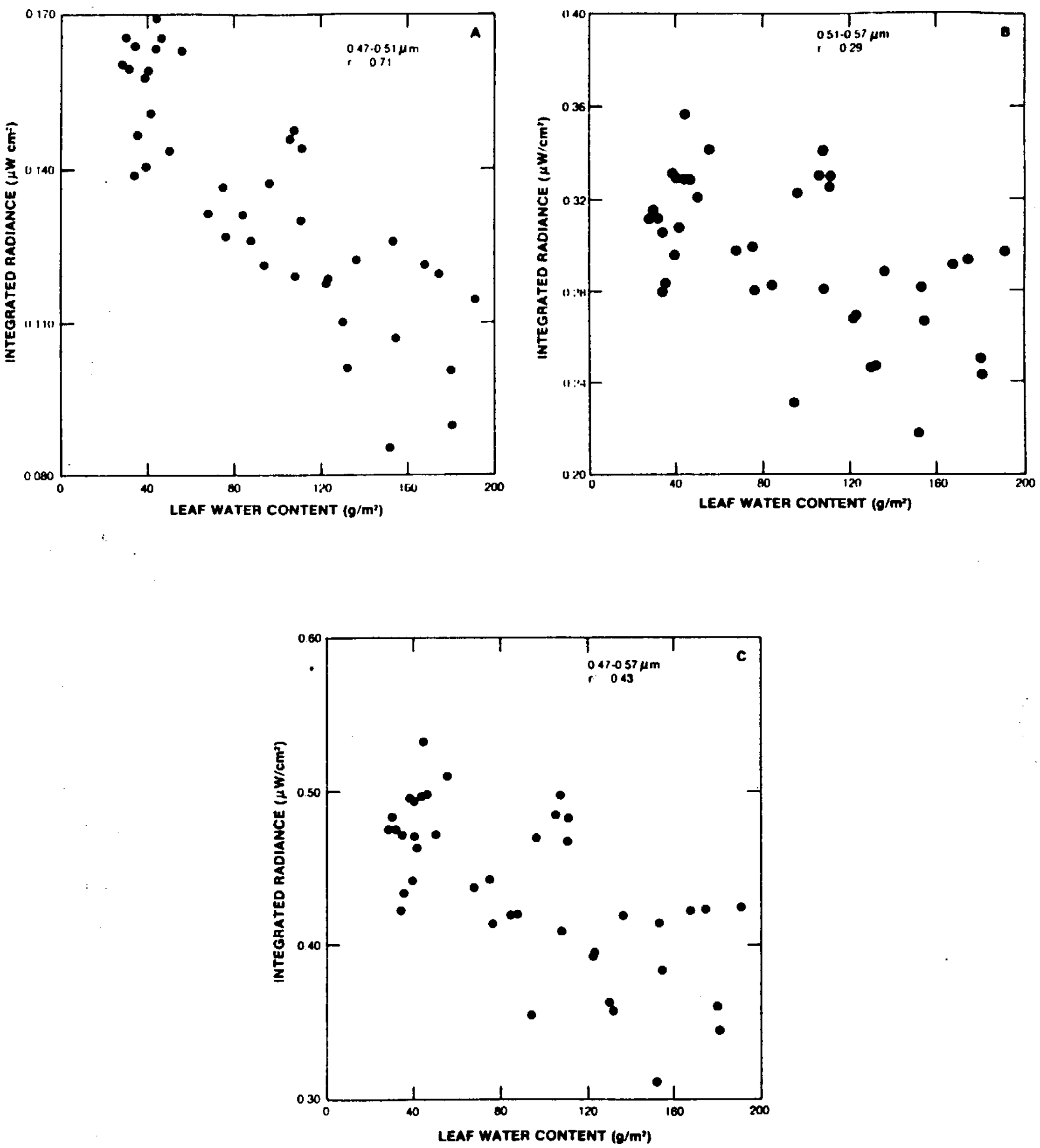

Figure 1. Integrated radiance for three wavelength intervals plotted against the leaf water content for the September sampling period. (A) 0.47 - 0.51 μm, (B) 0.51 - 0.57 μm, and (C) 0.47 - 0.57 μm. Note how two different effects occur within Colvocoresses' proposed band 1. The combination of these two wavelength regions seriously reduces the vegetational utility of this proposed sensor.

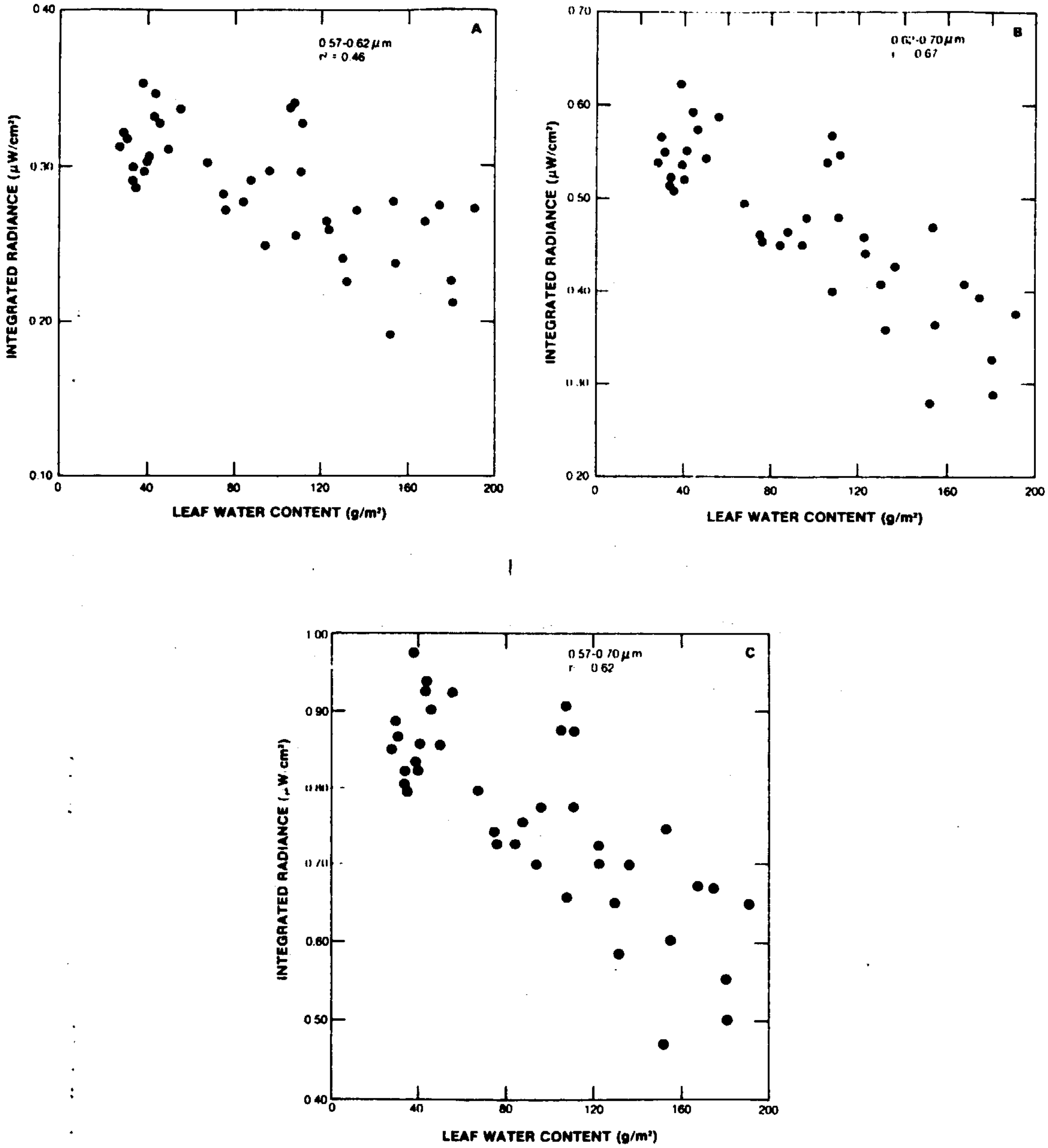

Figure 2. Integrated radiance for three wavelength intervals plotted against the leaf water content for the September sampling period. (A) 0.57 - 0.62 µm, (B) 0.62 - 0.70 µm, and (C) 0.57 - 0.70 µm. Note how two different effects occur with Colvocoresses' proposed band 2. This sensor could be improved for more complex vegetational utility by excluding the 0.57 - 0.62 µm region.

chlorophyll and carotenoid concentrations for the 0.45 - 0.50 μm region. In order to make this bandwidth wider to give more optimum signal/noise ratios, the bandwidth was widened on the upper end to 0.52 μm. It would be counterproductive to widen this sensor on the lower end (say to 0.43 μm) because of atmospheric scattering effects. TM1 thus is not optimum from a strictly spectral perspective but avoids potential signal/noise problems by including the 0.50 - 0.52 μm region.

TM2 (0.52 - 0.60 μm) is placed to record green region radiances. It is well situated to maximize the spectral information content but is not as highly correlated with green vegetation as are TM 1, TM 3, and TM 4. Sensor selection should attempt to place sensors in spectral regions where a particular relationship/process occurs to maximize the information content. It should not combine different relationships (see Table 2; Figures 1 and 2). TM2 is situated in a spectral region where a poor <u>per se</u> relationship holds between heterogeneous green vegetation and spectral reflectance (Table 5). This sensor receives other and potentially very valuable spectral information that is uncoupled from the more direct spectral-vegetational information present in the blue, red, and near infrared regions.

TM3 (0.63 - 0.69 μm) is well placed from a green vegetational perspective. It could be widened to 0.62 - 0.70 μm if additional signal were needed with a slight (1 - 3%) reduction in single channel utility. It is configured to be an excellent <u>in vivo</u> chlorophyll band (Tables 4 and 5).

TM4 (0.76 - 0.90 μm) is well situated from a spectral perspective related to green vegetation (Tables 4 and 5). TM4 excludes the 0.70 - 0.74 μm transition or noise region on its lower end and a 0.92 - 0.98 μm atmospheric water absorption band on its upper end. A previously published analysis has shown that this sensor combines excellent general vegetational application(s) with the ability to sense near-ir plateau rounding plant stress conditions within its 0.76 - 9.90 μm bandwidth (Tucker 1978). The wide bandwidth of TM4 coupled with the high levels of spectral reflectance characteristic of green vegetation for this region should result in optimal remote sensing of vegetational density for TM4. Avoiding the atmospheric water vapor absorption band in the 0.92 - 0.98 μm region will improve signature extension.

TM5 (1.55 - 1.75 μm) and TM6 (2.08 - 2.35 μm) could not be evaluated in this paper. However, both of these bands are directly sensitive to the leaf water content in terrestrial vegetation (Knipling, 1970; Woolley, 1971; Tucker and Garratt, 1977). Gausman et al. (1978) have reported excellent soil-green vegetation reflectance contrasts for these two wavebands. In addition to the vegetational utility in these two near infrared bands, other scientists have suggested geological applications (Abrams et al, 1977; Rowan et al, 1977).

SPOT

SPOT 1 (0.50 - 0.59 μm) is placed in sense green region spectral radiances (Tables 4 and 5). Slight pigment absorption may occur in the 0.50 - 0.52 μm region but this is a slight adjustment.

SPOT 2 (0.61 - 0.69 μm) is placed to sense spectral radiances highly correlated with the in vivo chlorophyll concentration(s) of green vegetation (Tables 4 and 5). A slight (1 - 2%) improvement in regression significance would result from excluding the 0.61 - 0.63 μm region at a sacrifice of the signal:noise ratio.

SPOT 3 (0.79 - 0.90 μm) is placed to sense spectral radiances which are highly correlated with green vegetational density (Table 4). No adjustments are suggested for this band.

In general, the SPOT bands are very similar from a spectral-vegetational perspective to thematic mapper bands TM2, TM3, and TM4. Both SPOT and the thematic mapper are optimally configured for the collection of remotely sensed data from green vegetation targets.

OUTLOOK FOR THE FUTURE

Substantial improvements over MSS imagery are expected from Landsat-D's thematic mapper as a result of spectral resolution alone. Coupled with increased radiometric resolution, increased spatial resolution, and additional bands, the state-of-the-art of satellite remote sensing of vegetated surfaces should be advanced dramatically.

In addition, the French SPOT satellite is promising from a spectral perspective and suggests a rational approach for a MLA "operational" system.

The next generation of satellite remote sensing is thus soon to begin. It will offer significant improvements in monitoring vegetation from orbital altitudes and demonstrate conclusively the many and varied applications of this technology.

CONCLUSIONS

1. Thematic Mapper sensors TM1, TM2, TM3, and TM4 were found to be very well situated for remote sensing of vegetated targets.

2. Significant improvements can be expected from the Thematic Mapper over the MSS of Landsats-1, 2, and 3, resulting from optimal spectral resolution alone.

3. Colvocoresses' proposed three band system was found to have two poor bands and one better band for monitoring vegetation. Thematic Mapper bands were found to be significantly superior to these proposed bands.

4. The French satellite SPOT three band system has three well placed bands for monitoring vegetation. The SPOT bands are very similar to Thematic Mapper bands TM2, TM3, and TM4, respectively.

5. Sensor bandwidths must be restricted to regions of the spectrum where the same vegetation-spectral reflectance relationship predominates. Combining different vegetation-spectral reflectance relationships within the same sensor bandwidth seriously reduced the vegetational utility of the "combined sensor" especially for more complex canopy situations.

6. Complex canopy situations necessitate a more specific spectral subset of the less complex canopy situation spectral regions. As such, the more heterogeneous or complex condition(s) are of predominant value for selecting sensors of the greatest and most persistent vegetational utility.

REFERENCES

Abrams, M. J., R. P. Ashley, L. C. Rowan, A. F. H. Goetz, and A. B. Kahle. 1977. Mapping of hydrothermal alteration in the Cuprite Mining District, Nevada, Using Aircraft Scanner Images for the Spectral Region of 0.46 - 2.36μm. Geology 5(12): 713-718.

CNES, 1978. Caracteristiques Principales du Satellite National d'Observation de la Terre: Project SPOT. Centre Spatial de Toulouse.

Colvocoresses, A. P. 1977. Proposed Parameters for an Operational Landsat. PE&RS 43(9): 1139-1145.

Deering, D. W. 1978. Rangeland Reflectance Characteristics Measured by aircraft and spacecraft sensors. PhD dissertation, Texas A&M Univ., College Station, 338 pp.

Draper, N. R. and H. Smith. 1966. Applied Regression Analysis. John Wiley and Sons, New York, 417 p.

Gausman, H. W., W. A. Allen, R. Cardenas, and A. J. Richardson. 1973. Reflectance Discrimination of Cotton and Corn at Four Growth Stages. Agron J. 65: 194-198.

Gausman, H. W., D. E. Escobar, J. H. Everitt, A. J. Richardson, and R. R. Rodriguez. 1978. Distinguishing succulent plants from crop and woody plants. PE&RS 44(4): 487-491.

Hovis, W. A. 1977. Personal communication to C. J. Tucker. NASA/GSFC.

Knipling, E. B., 1970. Physical and physiological basis for the reflectance of visible and near-infrared radiation from vegetation. RSE 1(3): 155-159.

Kondratyev, K. Y., O. B. Vassilyev, A. A. Grigoryev, and G. A. Ivanian. 1973. An analysis of the earth resources satellite (ERTS-1) data. RSE 2: 273-283.

Kondratyev, K. Y., A. A. Grigoryev, and O. M. Polioyskiy. 1975. Information content of the data obtained by remote sensing of the parameters of the environment and the earth's resources from space. Leningrad Univ. Press, Leningrad pp. 1 - 146 (NASA TT F 16435).

Maxwell, E. L. 1976. Multivariate system analysis of multispectral imagery. PE&RS 42(9): 1173-1186.

Miller, L. D., R. L. Pearson, and C. J. Tucker. 1976. Design of a mobile field spectrometer laboratory. PE&RS 42(4): 569-572.

NASA/GSFC 1973a. Symposium on Significant Results Obtained from ERTS-1. New Carrollton, Md. March 1973. NASA SP-327.

NASA/GSFC 1973b. Third Symposium on Significant Results Obtained from ERTS-1. Washington, D. C., December 1973. NASA SP-351.

National Research Council. 1976. Resource and Environmental Surveys from Space with the Thematic Mapper in the 1980's. National Academy of Science, NRC/CORSPERS - 76/1. Washington, D. C., 122 pp.

Rowan, L. C., A. H. Goetz, and R. P. Ashley. 1977. Discrimination of hydrothermally altered and unaltered rock in the visible and near infrared multispectral images. Geophysics 42(3): 522-535.

Rouse, J.W., R.H. Hass, J.A. Schell, D.W. Deering, and J.C. Harlan. 1974. Monitoring the vernai advancement and retrogradation (greenwave effect) of natural vegetation. Type III Final Report, NASA/GSFC, Greenbelt, MD. 342 p.

Salisbury, F.B. and C. Ross. 1969. Plant Physiology. Wadsworth Inc., Belmont California, 747 p.

Short, N.M., P.D. Lowman, S.C. Freden, and W.A. Finch. 1976. Mission to Earth: Landsat Views the World. NASA SP-360; QB637. M57, 459 p.

Tucker, C.J. 1978. The question of photographic infrared sensor redundancy for monitoring vegetation. PE&RS 44(3): 289-295.

Tucker, C.J. 1979. Red and photographic infrared linear combinations for monitoring vegetation. RSE (in press).

Tucker, C.J. and M.W. Garratt. 1977. Leaf optical system modeled as a stochastic process. Applied Optics 16(3): 635-642.

Tucker, C.J. 1977. Spectral estimation of grass canopy variables. RSE 6(1): 11-26.

Tucker, C.J. and E.L. Maxwell. 1976. Sensor design for monitoring vegetation canopies. PE&RS 42(11): 1399-1410.

Tucker, C.J. and L.D. Miller. 1977. Soil spectra contributions to grass canopy spectral reflectance. PE&RS 43(6): 721-726.

Williams, R.S., Jr. and W.D. Carter (eds.) 1976. ERTS-1: A New Window on our Planet. USGS professional paper 929, 362 p.

Woolley, J. T. 1971. Reflectance and transmittance of light by leaves. Plant Physiol. 47: 656–662.

APPENDIX A

CONTENTS

Appendix A contains tables corresponding to each of the sensors evaluated for the RBV, MSS, Thematic Mapper, Colvocoresses' operational Landsat three-band system, and the SPOT three-band system. Each sensor was evaluated by the following method: The upper wavelength limit of the sensor was held constant and the lower wavelength limit increased in 0.01 μm steps until the bandwidth was 0.01 μm wide. At each step, the respective bandwidth was integrated for each of the experimental spectral curves. Results were then regression screened to quantify the statistical significance between integrated radiance and the plot variable in question. Next, the lower wavelength limit was held constant and the upper limit decreased at 0.01 μm intervals until the bandwidth was 0.01 μm wide. The same analysis was performed on this set of data as the other.

The analysis was completed for all six of the plot variables. For the sake of concise presentation, however, only the total wet biomass results for the June data and the leaf water content results for the September data are presented. An explanation for this is given in the text.

Several other factors, conditions, etc. should be remembered when interpreting the within sensor tabular results presented in this appendix. Principal to these considerations are limitations in the data. The June spectral data, covering the ~0.35 - 0.80 μm (visible grating) and the 0.70 - 1.00 μm (infrared grating), suffers from a low signal/noise ratio in the ~0.35 - 0.46 μm region. For this reason, results from TM-1 are somewhat degraded as one can see in the respective Appendix A table. The rest of the June spectral data, covering the ~0.46 - 0.80 μm and the 0.70 - 1.00 μm intervals, are excellent data and do not suffer from the same condition.

The September spectral data, covering the 0.35 - 0.80 μm interval, suffers from lower signal/noise ratios in the ~0.35 - 0.36 μm and ~0.79 - 0.80 μm regions. This results from initial grating settings and/or the transducer coupling. The ~0.36 - 0.79 μm balance of the September spectral data is excellent, however.

There are, in addition, occasional glitches in the June and September spectral data corresponding to wavelengths where filter changes were made. These are not severe and are expressed as simply lower r^2 values relative to the adjacent higher r^2 values when the spectral data was regressed against the various plot variables. These types of data limitations are often impossible to avoid in field experiments and are noted here to explain what otherwise may be confusing in a small number of instances.

Table A1
Within Band Simulation Results for RBV-1. (A) is for 0.475 → 0.575 μm and (B) is for 0.475 ← 0.575 μm

June (n = 35)			September (n = 40)		
Rank	Ordered r^2's	Wavelength (μm)	Rank	Ordered r^2's	Wavelength (μm)
A					
1	0.73	0.475 - 0.575	1	0.41	0.475 - 0.575
2	0.72	0.545 - 0.575	2	0.38	0.485 - 0.575
3	0.71	0.535 - 0.575	3	0.35	0.495 - 0.575
4	0.71	0.555 - 0.575	4	0.31	0.505 - 0.575
5	0.70	0.485 - 0.575	5	0.29	0.565 - 0.575
6	0.70	0.525 - 0.575	6	0.28	0.515 - 0.575
7	0.68	0.515 - 0.575	7	0.25	0.525 - 0.575
8	0.68	0.495 - 0.575	8	0.25	0.555 - 0.575
9	0.66	0.505 - 0.575	9	0.24	0.535 - 0.575
10	0.62	0.565 - 0.575	10	0.24	0.545 - 0.575
B					
1	0.83	0.475 - 0.485	1	0.72	0.475 - 0.495
2	0.82	0.475 - 0.495	2	0.72	0.475 - 0.505
3	0.79	0.475 - 0.505	3	0.70	0.475 - 0.485
4	0.75	0.475 - 0.515	4	0.68	0.475 - 0.515
5	0.73	0.475 - 0.525	5	0.64	0.475 - 0.525
6	0.73	0.475 - 0.575	6	0.58	0.475 - 0.535
7	0.72	0.475 - 0.565	7	0.52	0.475 - 0.545
8	0.72	0.475 - 0.535	8	0.47	0.475 - 0.555
9	0.72	0.475 - 0.555	9	0.43	0.475 - 0.565
10	0.72	0.475 - 0.545	10	0.41	0.475 - 0.575

Table A2
Within Band Simulation Results for RBV-2. (A) is for $0.58 \rightarrow 0.68\mu m$ and (B) is for $0.58 \leftarrow 0.68\mu m$

June (n = 35)			September (n = 40)		
Rank	Ordered r^2's	Wavelength (μm)	Rank	Ordered r^2's	Wavelength (μm)
A					
1	0.93	0.67 - 0.68	1	0.74	0.67 - 0.68
2	0.93	0.66 - 0.68	2	0.73	0.66 - 0.68
3	0.93	0.65 - 0.68	3	0.73	0.65 - 0.68
4	0.88	0.58 - 0.68	4	0.72	0.64 - 0.68
5	0.88	0.59 - 0.68	5	0.71	0.63 - 0.68
6	0.88	0.60 - 0.68	6	0.70	0.62 - 0.68
7	0.88	0.61 - 0.68	7	0.69	0.61 - 0.68
8	0.88	0.62 - 0.68	8	0.67	0.60 - 0.68
9	0.87	0.63 - 0.68	9	0.65	0.59 - 0.68
10	0.86	0.64 - 0.68	10	0.64	0.58 - 0.68
B					
1	0.89	0.58 - 0.64	1	0.64	0.58 - 0.68
2	0.88	0.58 - 0.62	2	0.62	0.58 - 0.67
3	0.88	0.58 - 0.63	3	0.60	0.58 - 0.66
4	0.88	0.58 - 0.68	4	0.57	0.58 - 0.65
5	0.88	0.58 - 0.61	5	0.54	0.58 - 0.64
6	0.88	0.58 - 0.67	6	0.51	0.58 - 0.63
7	0.87	0.58 - 0.60	7	0.48	0.58 - 0.62
8	0.87	0.58 - 0.59	8	0.44	0.58 - 0.61
9	0.87	0.58 - 0.66	9	0.43	0.58 - 0.60
10	0.85	0.58 - 0.65	10	0.42	0.58 - 0.59

Table A3
Within Band Simulation Results for RBV-3. (A) is for 0.69 → 0.80 μm and (B) is for 0.69 ← 0.80 μm

June (n = 35)			September (n = 40)		
Rank	Ordered r^2's	Wavelength (μm)	Rank	Ordered r^2's	Wavelength (μm)
A					
1	0.83	0.75 - 0.80	1	0.68	0.76 - 0.80
2	0.82	0.76 - 0.80	2	0.68	0.75 - 0.80
3	0.82	0.74 - 0.80	3	0.66	0.74 - 0.80
4	0.82	0.77 - 0.80	4	0.63	0.73 - 0.80
5	0.81	0.73 - 0.80	5	0.63	0.77 - 0.80
6	0.80	0.78 - 0.80	6	0.59	0.72 - 0.80
7	0.80	0.79 - 0.80	7	0.54	0.71 - 0.80
8	0.78	0.72 - 0.80	8	0.54	0.78 - 0.80
9	0.74	0.71 - 0.80	9	0.48	0.70 - 0.80
10	0.70	0.70 - 0.80	10	0.47	0.79 - 0.80
11	0.65	0.69 - 0.80	11	0.41	0.69 - 0.80
B					
1	0.65	0.69 - 0.80	1	0.50	0.69 - 0.70
2	0.60	0.69 - 0.79	2	0.41	0.69 - 0.80
3	0.59	0.69 - 0.70	3	0.40	0.69 - 0.79
4	0.54	0.69 - 0.71	4	0.37	0.69 - 0.71
5	0.53	0.69 - 0.78	5	0.35	0.69 - 0.78
6	0.43	0.69 - 0.72	6	0.29	0.69 - 0.72
7	0.43	0.69 - 0.77	7	0.25	0.69 - 0.77
8	0.28	0.69 - 0.76	8	0.18	0.69 - 0.73
9	0.20	0.69 - 0.73	9	0.10	0.69 - 0.76
10	0.08	0.69 - 0.75	10	0.04	0.69 - 0.74
11	0.01	0.69 - 0.74	11	0.01	0.69 - 0.75

Table A4
Within Band Simulation Results for MSS-4. (A) is for $0.50 \rightarrow 0.60 \mu m$ and (B) is for $0.50 \leftarrow 0.60 \mu m$

June (n = 35)			September (n = 40)		
Rank	Ordered r^2's	Wavelength (μm)	Rank	Ordered r^2's	Wavelength (μm)
A					
1	0.87	0.59 - 0.60	1	0.43	0.59 - 0.60
2	0.87	0.58 - 0.60	2	0.43	0.58 - 0.60
3	0.86	0.57 - 0.60	3	0.40	0.57 - 0.60
4	0.85	0.56 - 0.60	4	0.37	0.56 - 0.60
5	0.84	0.55 - 0.60	5	0.37	0.50 - 0.60
6	0.83	0.54 - 0.60	6	0.34	0.51 - 0.60
7	0.80	0.53 - 0.60	7	0.34	0.55 - 0.60
8	0.79	0.52 - 0.60	8	0.33	0.54 - 0.60
9	0.78	0.51 - 0.60	9	0.33	0.52 - 0.60
10	0.78	0.50 - 0.60	10	0.32	0.53 - 0.60
B					
1	0.78	0.50 - 0.60	1	0.64	0.50 - 0.51
2	0.76	0.50 - 0.59	2	0.59	0.50 - 0.52
3	0.73	0.50 - 0.58	3	0.52	0.50 - 0.53
4	0.70	0.50 - 0.57	4	0.44	0.50 - 0.54
5	0.68	0.50 - 0.51	5	0.39	0.50 - 0.55
6	0.67	0.50 - 0.52	6	0.37	0.50 - 0.60
7	0.67	0.50 - 0.56	7	0.35	0.50 - 0.56
8	0.65	0.50 - 0.53	8	0.35	0.50 - 0.59
9	0.63	0.50 - 0.55	9	0.33	0.50 - 0.58
10	0.62	0.50 - 0.54	10	0.33	0.50 - 0.57

Table A5
Within Band Simulation Results for MSS-5. (A) is for $0.60 \rightarrow 0.70\mu m$ and (B) is for $0.60 \leftarrow 0.70\mu m$

June (n = 35)			September (n = 40)		
Rank	Ordered r^2's	Wavelength (μm)	Rank	Ordered r^2's	Wavelength (μm)
A					
1	0.90	0.65 - 0.70	1	0.68	0.64 - 0.70
2	0.89	0.66 - 0.70	2	0.68	0.63 - 0.70
3	0.88	0.60 - 0.70	3	0.67	0.62 - 0.70
4	0.88	0.61 - 0.70	4	0.67	0.65 - 0.70
5	0.87	0.62 - 0.70	5	0.66	0.61 - 0.70
6	0.87	0.63 - 0.70	6	0.66	0.66 - 0.70
7	0.87	0.67 - 0.70	7	0.65	0.60 - 0.70
8	0.87	0.64 - 0.70	8	0.63	0.67 - 0.70
9	0.83	0.68 - 0.70	9	0.56	0.68 - 0.70
10	0.77	0.69 - 0.70	10	0.50	0.69 - 0.70
B					
1	0.89	0.60 - 0.62	1	0.67	0.60 - 0.68
2	0.89	0.60 - 0.64	2	0.67	0.60 - 0.69
3	0.89	0.60 - 0.61	3	0.65	0.60 - 0.67
4	0.89	0.60 - 0.63	4	0.65	0.60 - 0.70
5	0.89	0.60 - 0.69	5	0.63	0.60 - 0.66
6	0.88	0.60 - 0.68	6	0.61	0.60 - 0.65
7	0.88	0.60 - 0.70	7	0.58	0.60 - 0.64
8	0.87	0.60 - 0.67	8	0.55	0.60 - 0.63
9	0.86	0.60 - 0.66	9	0.52	0.60 - 0.62
10	0.84	0.60 - 0.65	10	0.46	0.60 - 0.61

Table A6
Within Band Simulation Results for MSS-6. (A) is for $0.70 \rightarrow 0.80\mu m$ and (B) is for $0.70 \leftarrow 0.80\mu m$

June (n = 35)			September (n = 40)		
Rank	Ordered r^2's	Wavelength (μm)	Rank	Ordered r^2's	Wavelength (μm)
A					
1	0.83	0.75 - 0.80	1	0.68	0.76 - 0.80
2	0.82	0.76 - 0.80	2	0.68	0.75 - 0.80
3	0.82	0.74 - 0.80	3	0.66	0.74 - 0.80
4	0.82	0.77 - 0.80	4	0.63	0.73 - 0.80
5	0.81	0.73 - 0.80	5	0.63	0.77 - 0.80
6	0.80	0.78 - 0.80	6	0.59	0.72 - 0.80
7	0.80	0.79 - 0.80	7	0.54	0.71 - 0.80
8	0.78	0.72 - 0.80	8	0.54	0.78 - 0.80
9	0.74	0.71 - 0.80	9	0.48	0.70 - 0.80
10	0.70	0.70 - 0.80	10	0.47	0.79 - 0.80
B					
1	0.70	0.70 - 0.80	1	0.48	0.70 - 0.80
2	0.66	0.70 - 0.79	2	0.48	0.70 - 0.79
3	0.61	0.70 - 0.78	3	0.45	0.70 - 0.78
4	0.52	0.70 - 0.77	4	0.36	0.70 - 0.77
5	0.49	0.70 - 0.71	5	0.25	0.70 - 0.71
6	0.40	0.70 - 0.76	6	0.21	0.70 - 0.76
7	0.34	0.70 - 0.72	7	0.18	0.70 - 0.72
8	0.20	0.70 - 0.75	8	0.07	0.70 - 0.73
9	0.10	0.70 - 0.73	9	0.07	0.70 - 0.75
10	0.01	0.70 - 0.74	10	0.00	0.70 - 0.74

Table A7
Within Band Simulation Results for MSS-7 for the June Infrared Data (n = 33). (A) is for 0.80→1.00 μm and (B) is for 0.80←1.00 μm. The upper wave-length limit of 1.00 was used because MSS-7 receives porportionally little signal from the 1.00 - 1.10 μm region relative to that of the 0.80 - 1.00 μm region (Hovis 1977).

A			B		
Rank	Ordered r^2's	Wavelength (μm)	Rank	Ordered r^2's	Wavelength (μm)
1	0.72	0.80 - 1.00	1	0.78	0.80 - 0.82
2	0.72	0.81 - 1.00	2	0.78	0.80 - 0.81
3	0.72	0.82 - 1.00	3	0.78	0.80 - 0.83
4	0.71	0.83 - 1.00	4	0.77	0.80 - 0.84
5	0.71	0.84 - 1.00	5	0.77	0.80 - 0.85
6	0.71	0.85 - 1.00	6	0.75	0.80 - 0.86
7	0.70	0.86 - 1.00	7	0.75	0.80 - 0.87
8	0.69	0.87 - 1.00	8	0.75	0.80 - 0.88
9	0.68	0.88 - 1.00	9	0.75	0.80 - 0.89
10	0.67	0.89 - 1.00	10	0.75	0.80 - 0.90
11	0.66	0.90 - 1.00	11	0.75	0.80 - 0.91
12	0.65	0.91 - 1.00	12	0.75	0.80 - 0.92
13	0.63	0.92 - 1.00	13	0.75	0.80 - 0.93
14	0.61	0.93 - 1.00	14	0.74	0.80 - 0.94
15	0.59	0.94 - 1.00	15	0.74	0.80 - 0.95
16	0.57	0.95 - 1.00	16	0.73	0.80 - 0.96
17	0.54	0.96 - 1.00	17	0.73	0.80 - 0.97
18	0.49	0.97 - 1.00	18	0.72	0.80 - 0.98
19	0.40	0.98 - 1.00	19	0.72	0.80 - 0.99
20	0.33	0.99 - 1.00	20	0.72	0.80 - 1.00

Table A8

Within Band Simulation Results for TM-1. (A) is for 0.45 → 0.52 μm and (B) is for 0.45 ← 0.52 μm

June (n = 35)			September (n = 40)		
Rank	Ordered r^2's	Wavelength (μm)	Rank	Ordered r^2's	Wavelength (μm)
A					
1	0.71	0.48 - 0.52	1	0.69	0.45 - 0.52
2	0.70	0.47 - 0.52	2	0.68	0.46 - 0.52
3	0.70	0.46 - 0.52	3	0.67	0.47 - 0.52
4	0.69	0.49 - 0.52	4	0.66	0.48 - 0.52
5	0.69	0.45 - 0.52	5	0.63	0.49 - 0.52
6	0.67	0.50 - 0.52	6	0.59	0.50 - 0.52
7	0.65	0.51 - 0.52	7	0.52	0.51 - 0.52
B					
1	0.69	0.45 - 0.51	1	0.73	0.45 - 0.50
2	0.69	0.45 - 0.52	2	0.72	0.45 - 0.49
3	0.69	0.45 - 0.50	3	0.72	0.45 - 0.51
4	0.66	0.45 - 0.49	4	0.71	0.45 - 0.47
5	0.63	0.45 - 0.48	5	0.71	0.45 - 0.48
6	0.58	0.45 - 0.47	6	0.69	0.45 - 0.52
7	0.55	0.45 - 0.46	7	0.68	0.45 - 0.46

Table A9
Within Band Simulation Results for TM-2. (A) is for 0.52 → 0.60 μm and (B) is for 0.52 ← 0.60 μm

June (n = 35)			September (n = 40)		
Rank	Ordered r^2's	Wavelength (μm)	Rank	Ordered r^2's	Wavelength (μm)
A					
1	0.87	0.59 - 0.60	1	0.43	0.59 - 0.60
2	0.87	0.58 - 0.60	2	0.43	0.58 - 0.60
3	0.86	0.57 - 0.60	3	0.40	0.57 - 0.60
4	0.85	0.56 - 0.60	4	0.37	0.56 - 0.60
5	0.84	0.55 - 0.60	5	0.34	0.55 - 0.60
6	0.83	0.54 - 0.60	6	0.33	0.54 - 0.60
7	0.80	0.53 - 0.60	7	0.33	0.52 - 0.60
8	0.79	0.52 - 0.60	8	0.32	0.53 - 0.60
B					
1	0.79	0.52 - 0.60	1	0.37	0.52 - 0.53
2	0.77	0.52 - 0.59	2	0.33	0.52 - 0.60
3	0.74	0.52 - 0.58	3	0.30	0.52 - 0.59
4	0.70	0.52 - 0.57	4	0.30	0.52 - 0.54
5	0.66	0.52 - 0.56	5	0.27	0.52 - 0.58
6	0.61	0.52 - 0.55	6	0.27	0.52 - 0.55
7	0.61	0.52 - 0.54	7	0.26	0.52 - 0.56
8	0.56	0.52 - 0.53	8	0.25	0.52 - 0.57

Table A10
Within Band Simulation Results for TM-3. (A) is for $0.63 \rightarrow 0.69 \mu m$ and (B) is for $0.63 \leftarrow 0.69 \mu m$

June (n = 35)			September (n = 40)		
Rank	Ordered r^2's	Wavelength (μm)	Rank	Ordered r^2's	Wavelength (μm)
A					
1	0.92	0.65 - 0.69	1	0.71	0.64 - 0.69
2	0.91	0.66 - 0.69	2	0.71	0.65 - 0.69
3	0.91	0.67 - 0.69	3	0.70	0.66 - 0.69
4	0.88	0.68 - 0.69	4	0.70	0.63 - 0.69
5	0.88	0.63 - 0.69	5	0.69	0.67 - 0.69
6	0.87	0.64 - 0.69	6	0.62	0.68 - 0.69
B					
1	0.89	0.63 - 0.64	1	0.71	0.63 - 0.68
2	0.88	0.63 - 0.69	2	0.70	0.63 - 0.69
3	0.87	0.63 - 0.68	3	0.70	0.63 - 0.67
4	0.85	0.63 - 0.67	4	0.69	0.63 - 0.66
5	0.81	0.63 - 0.66	5	0.67	0.63 - 0.65
6	0.74	0.63 - 0.65	6	0.62	0.63 - 0.64

Table A11

Within Band Simulation Results for TM-4 for the June Infrared Data (n = 33). (A) is for 0.76 → 0.90 μm and (B) is for 0.76 ← 0.90 μm

Rank	Ordered r^2's	Wavelength (μm)	Rank	Ordered r^2's	Wavelength (μm)
A			B		
1	0.78	0.76 - 0.90	1	0.80	0.76 - 0.77
2	0.78	0.77 - 0.90	2	0.80	0.76 - 0.78
3	0.78	0.78 - 0.90	3	0.80	0.76 - 0.80
4	0.77	0.79 - 0.90	4	0.80	0.76 - 0.79
5	0.77	0.80 - 0.90	5	0.79	0.76 - 0.81
6	0.77	0.81 - 0.90	6	0.79	0.76 - 0.82
7	0.77	0.85 - 0.90	7	0.79	0.76 - 0.83
8	0.77	0.82 - 0.90	8	0.79	0.76 - 0.84
9	0.77	0.83 - 0.90	9	0.78	0.76 - 0.85
10	0.76	0.84 - 0.90	10	0.78	0.76 - 0.86
11	0.76	0.86 - 0.90	11	0.78	0.76 - 0.87
12	0.76	0.87 - 0.90	12	0.78	0.76 - 0.88
13	0.76	0.88 - 0.90	13	0.78	0.76 - 0.89
14	0.75	0.89 - 0.90	14	0.78	0.76 - 0.90

Table A12
Within Band Simulation Results for Colvocoresses' Band-1. (A) is for 0.47 → 0.57 μm and (B) is for 0.47 ← 0.57 μm

June (n = 35)			September (n = 40)		
Rank	Ordered r^2's	Wavelength (μm)	Rank	Ordered r^2's	Wavelength (μm)
A					
1	0.81	0.56 - 0.57	1	0.43	0.47 - 0.57
2	0.79	0.55 - 0.57	2	0.40	0.48 - 0.57
3	0.76	0.54 - 0.57	3	0.37	0.49 - 0.57
4	0.72	0.53 - 0.57	4	0.33	0.50 - 0.57
5	0.71	0.47 - 0.57	5	0.29	0.51 - 0.57
6	0.71	0.48 - 0.57	6	0.25	0.52 - 0.57
7	0.71	0.49 - 0.57	7	0.23	0.56 - 0.57
8	0.70	0.52 - 0.57	8	0.23	0.53 - 0.57
9	0.70	0.50 - 0.57	9	0.22	0.54 - 0.57
10	0.70	0.51 - 0.57	10	0.21	0.55 - 0.57
B					
1	0.71	0.47 - 0.50	1	0.73	0.47 - 0.50
2	0.71	0.47 - 0.51	2	0.72	0.47 - 0.49
3	0.71	0.47 - 0.57	3	0.71	0.47 - 0.51
4	0.70	0.47 - 0.52	4	0.69	0.47 - 0.48
5	0.69	0.47 - 0.53	5	0.67	0.47 - 0.52
6	0.69	0.47 - 0.56	6	0.62	0.47 - 0.53
7	0.69	0.47 - 0.49	7	0.56	0.47 - 0.54
8	0.67	0.47 - 0.55	8	0.51	0.47 - 0.55
9	0.67	0.47 - 0.54	9	0.46	0.47 - 0.56
10	0.60	0.47 - 0.48	10	0.43	0.47 - 0.57

Table A13
Within Band Simulation Results for Colvocoresses' Band-2. (A) is for $0.57 \rightarrow 0.70 \mu m$ and (B) is for $0.57 \leftarrow 0.70 \mu m$

June (n = 35)			September (n = 40)		
Rank	Ordered r^2's	Wavelength (μm)	Rank	Ordered r^2's	Wavelength (μm)
A					
1	0.90	0.65 - 0.70	1	0.68	0.64 - 0.70
2	0.89	0.66 - 0.70	2	0.68	0.63 - 0.70
3	0.88	0.58 - 0.70	3	0.67	0.62 - 0.70
4	0.88	0.60 - 0.70	4	0.67	0.65 - 0.70
5	0.88	0.59 - 0.70	5	0.66	0.61 - 0.70
6	0.88	0.57 - 0.70	6	0.66	0.66 - 0.70
7	0.88	0.61 - 0.70	7	0.65	0.60 - 0.70
8	0.87	0.62 - 0.70	8	0.64	0.59 - 0.70
9	0.87	0.63 - 0.70	9	0.63	0.67 - 0.70
10	0.87	0.67 - 0.70	10	0.63	0.58 - 0.70
11	0.87	0.64 - 0.70	11	0.62	0.57 - 0.70
12	0.83	0.68 - 0.70	12	0.56	0.68 - 0.70
13	0.77	0.69 - 0.70	13	0.50	0.69 - 0.70
B					
1	0.88	0.57 - 0.69	1	0.62	0.57 - 0.69
2	0.88	0.57 - 0.64	2	0.62	0.57 - 0.68
3	0.88	0.57 - 0.68	3	0.62	0.57 - 0.70
4	0.88	0.57 - 0.63	4	0.60	0.57 - 0.67
5	0.88	0.57 - 0.62	5	0.58	0.57 - 0.66
6	0.88	0.57 - 0.70	6	0.55	0.57 - 0.65
7	0.88	0.57 - 0.67	7	0.53	0.57 - 0.64
8	0.87	0.57 - 0.61	8	0.49	0.57 - 0.63
9	0.87	0.57 - 0.66	9	0.46	0.57 - 0.62
10	0.86	0.57 - 0.60	10	0.43	0.57 - 0.61
11	0.86	0.57 - 0.59	11	0.40	0.57 - 0.60
12	0.85	0.57 - 0.65	12	0.38	0.57 - 0.59
13	0.85	0.57 - 0.58	13	0.34	0.57 - 0.58

Table A14

Within Band Simulation Results for Colvocoresses' Band-3 for the June Infrared Data (n = 33). (A) is for 0.76 → 1.00 μm and (B) is for 0.76 ← 1.00 μm. The upper limit of 1.00 μm was used for these simulations instead of 1.05 μm.

A			B		
Rank	Ordered r^2's	Wavelength (μm)	Rank	Ordered r^2's	Wavelength (μm)
1	0.74	0.76 - 1.00	1	0.80	0.76 - 0.77
2	0.74	0.77 - 1.00	2	0.80	0.76 - 0.78
3	0.74	0.78 - 1.00	3	0.80	0.76 - 0.80
4	0.73	0.79 - 1.00	4	0.80	0.76 - 0.79
5	0.72	0.80 - 1.00	5	0.79	0.76 - 0.81
6	0.72	0.81 - 1.00	6	0.79	0.76 - 0.82
7	0.72	0.82 - 1.00	7	0.79	0.76 - 0.83
8	0.71	0.83 - 1.00	8	0.79	0.76 - 0.84
9	0.71	0.84 - 1.00	9	0.78	0.76 - 0.85
10	0.71	0.85 - 1.00	10	0.78	0.76 - 0.86
11	0.70	0.86 - 1.00	11	0.78	0.76 - 0.87
12	0.69	0.87 - 1.00	12	0.78	0.76 - 0.88
13	0.68	0.88 - 1.00	13	0.78	0.76 - 0.89
14	0.67	0.89 - 1.00	14	0.78	0.76 - 0.90
15	0.66	0.90 - 1.00	15	0.78	0.76 - 0.91
16	0.65	0.91 - 1.00	16	0.78	0.76 - 0.92
17	0.63	0.92 - 1.00	17	0.77	0.76 - 0.93
18	0.61	0.93 - 1.00	18	0.77	0.76 - 0.94
19	0.59	0.94 - 1.00	19	0.77	0.76 - 0.95
20	0.57	0.95 - 1.00	20	0.76	0.76 - 0.96
21	0.54	0.96 - 1.00	21	0.76	0.76 - 0.97
22	0.49	0.97 - 1.00	22	0.75	0.76 - 0.98
23	0.40	0.98 - 1.00	23	0.75	0.76 - 0.99
24	0.33	0.99 - 1.00	24	0.74	0.76 - 1.00

Table A15

Within Band Simulation Results for SPOT-1. (A) is for 0.50→0.59 μm and (B) is for 0.50←0.59 μm.

June (n = 35)			September (n = 40)		
Rank	Ordered r^2's	Wavelength (μm)	Rank	Ordered r^2's	Wavelength (μm)
A					
1	0.87	0.58 - 0.59	1	0.42	0.58 - 0.59
2	0.86	0.57 - 0.59	2	0.38	0.57 - 0.59
3	0.85	0.56 - 0.59	3	0.35	0.50 - 0.59
4	0.83	0.55 - 0.59	4	0.34	0.56 - 0.59
5	0.81	0.54 - 0.59	5	0.32	0.51 - 0.59
6	0.78	0.53 - 0.59	6	0.31	0.55 - 0.59
7	0.77	0.52 - 0.59	7	0.30	0.52 - 0.59
8	0.76	0.51 - 0.59	8	0.30	0.54 - 0.59
9	0.76	0.50 - 0.59	9	0.29	0.53 - 0.59
B					
1	0.76	0.50 - 0.59	1	0.64	0.50 - 0.51
2	0.73	0.50 - 0.58	2	0.59	0.50 - 0.52
3	0.70	0.50 - 0.57	3	0.52	0.50 - 0.53
4	0.68	0.50 - 0.51	4	0.44	0.50 - 0.54
5	0.67	0.50 - 0.52	5	0.39	0.50 - 0.55
6	0.67	0.50 - 0.56	6	0.35	0.50 - 0.56
7	0.65	0.50 - 0.53	7	0.35	0.50 - 0.59
8	0.63	0.50 - 0.55	8	0.33	0.50 - 0.58
9	0.62	0.50 - 0.54	9	0.33	0.50 - 0.57

Table A16

Within Band Simulation Results for SPOT-2. (A) is for 0.61 → 0.69 μm and (B) is for 0.61 ← 0.69 μm.

June (n = 35)			September (n = 40)		
Rank	Ordered r^2's	Wavelength (μm)	Rank	Ordered r^2's	Wavelength (μm)
A					
1	0.92	0.65 - 0.69	1	0.71	0.64 - 0.69
2	0.91	0.66 - 0.69	2	0.71	0.65 - 0.69
3	0.91	0.67 - 0.69	3	0.70	0.66 - 0.69
4	0.88	0.61 - 0.69	4	0.70	0.63 - 0.69
5	0.88	0.62 - 0.69	5	0.69	0.62 - 0.69
6	0.88	0.68 - 0.69	6	0.69	0.67 - 0.69
7	0.88	0.63 - 0.69	7	0.68	0.61 - 0.69
8	0.87	0.64 - 0.69	8	0.62	0.68 - 0.69
B					
1	0.89	0.61 - 0.62	1	0.69	0.61 - 0.68
2	0.89	0.61 - 0.64	2	0.68	0.61 - 0.69
3	0.89	0.61 - 0.63	3	0.67	0.61 - 0.67
4	0.88	0.61 - 0.69	4	0.65	0.61 - 0.66
5	0.88	0.61 - 0.68	5	0.63	0.61 - 0.65
6	0.87	0.61 - 0.67	6	0.61	0.61 - 0.64
7	0.85	0.61 - 0.66	7	0.58	0.61 - 0.63
8	0.82	0.61 - 0.65	8	0.55	0.61 - 0.62

Table A17

Within Band Simulation Results for SPOT-3 for the June Infrared Data (n = 33). (A) is for 0.79 → 0.90 μm and (B) is for 0.79 ← 0.90 μm.

A			B		
Rank	Ordered r^2's	Wavelength (μm)	Rank	Ordered r^2's	Wavelength (μm)
1	0.77	0.79 - 0.90	1	0.80	0.79 - 0.80
2	0.77	0.80 - 0.90	2	0.79	0.79 - 0.81
3	0.77	0.81 - 0.90	3	0.79	0.79 - 0.82
4	0.77	0.82 - 0.90	4	0.78	0.79 - 0.83
5	0.77	0.83 - 0.90	5	0.78	0.79 - 0.84
6	0.77	0.84 - 0.90	6	0.78	0.79 - 0.85
7	0.76	0.85 - 0.90	7	0.78	0.79 - 0.86
8	0.76	0.86 - 0.90	8	0.78	0.79 - 0.87
9	0.76	0.87 - 0.90	9	0.78	0.79 - 0.88
10	0.76	0.88 - 0.90	10	0.77	0.79 - 0.89
11	0.75	0.89 - 0.90	11	0.77	0.79 - 0.90

BIBLIOGRAPHIC DATA SHEET

1. Report No.	2. Government Accession No.	3. Recipient's Catalog No.
4. Title and Subtitle An Evaluation of the 1st 4 Landsat-D Reflective Sensors for Monitoring Vegetation: A Comparison with Other Satellite Sensor Systems.		5. Report Date 6. Performing Organization Code
7. Author(s) C. J. Tucker		8. Performing Organization Report No.
9. Performing Organization Name and Address Code 923 NASA/GSFC		10. Work Unit No. 11. Contract or Grant No.
12. Sponsoring Agency Name and Address Code 923 NASA/GSFC		13. Type of Report and Period Covered 14. Sponsoring Agency Code
15. Supplementary Notes None		

16. Abstract

The first four Landsat-D thematic mapper sensors were evaluated and compared to: the RBV and MSS sensors from Landsats-1, 2, and 3; Colvocoresses' proposed "operational Landsat" three band system; and the French SPOT three band system using stimulation/integration techniques and in situ collected spectral reflectance data. Sensors were evaluated by their ability to discriminate vegetation biomass, chlorophyll concentration, and leaf water content. The thematic mapper and SPOT bands were found to be superior in a spectral resolution context to the other three sensor systems for vegetational applications. Significant improvements are expected for most vegetational analyses from Landsat-D thematic mapper and SPOT imagery over MSS and RBV imagery.

17. Key Words (Selected by Author(s))	18. Distribution Statement		
Remote Sensing of Vegetation Spectral Measurements, Landsat-D			
19. Security Classif. (of this report)	20. Security Classif. (of this page)	21. No. of Pages	22. Price*

*For sale by the National Technical Information Service, Springfield, Virginia 22151.

GSFC 25-44 (10/77)